PHYSICS AND CHEMISTRY OF SOLID STATE
V. 27, No. 2 (2026) pp. 227-241
Section: Physics

DOI: 10.15330/pcss.27.2.227-241

Vasyl Stefanyk Carpathian National University

ФІЗИКА І ХІМІЯ ТВЕРДОГО ТІЛА
Т. 27, № 2 (2026) С. 227-241
Фізико-математичні науки

PACS: 33.80.Eh, 61.46.+w

ISSN 1729-4428 (Print)
ISSN 2309-8589 (Online)

Santanu Kumar Nayak, Padmaja Patnaik, Dipan Kumar Das, Mandakini Baral

Enhancing ZnO: A Comprehensive Review of Group-III Element Doping Strategies and Applications

Centurion University of Technology and Management, Odisha, India, padmaja.patnaik@gmail.com

Wide bandgap semiconductors like Zinc oxide (ZnO) have potential applications in energy storage devices, optoelectronics, gas sensor etc. However, the inherent restrictions on electrical conductivity and bandgap required tactical adjustments. Group-III element doping has come to light as a viable strategy for overcoming these obstacles. Electronic properties of ZnO, such as band gap, density of states (DOS), partial density of states (PDOS), magnetic properties and optical properties like conductivity, dielectric loss, reflectivity, transparency, absorbance etc., are calculated utilizing *first principle* density functional theory.

This review article focused the recently development in the field of ZnO and group-III elements (B, Al, Ga, In) doped ZnO, it also highlights various potential applications of ZnO including light emitting diodes (LED_s), gas sensing, piezoelectric devices, solar cell etc. several number of approaches with varying approximations were carried out to investigate the structural, electronic and optical properties of intrinsic and group-III element doped ZnO.

Keywords: ZnO, group III, band gap, DFT, First principle.

Received 17 January 2025; Accepted 23 March 2026, Published 11 April 2026.

Content

Introduction

Zinc oxide (ZnO), a wide band gap semiconductor material exhibit band gap around 3.4 eV and at room temperature and exhibits significant binding energy (60 meV) [1] and highly transparent in visible light region [2] with a variety of important applications in optoelectronics, Photocatalyst [3], photoelectric applications like transparent conducting oxide (TCO),

sensing [4], light emitting diode (LED) [5,6], solar cell [7] and piezoelectric devices[8]. Due to the versatility of ZnO, it has several possible applications in the variety of industries including electronics, opto-electronics, catalysis and medicine. ZnO exhibit some unique characteristics such as high thermal stability which is useful for high temperature application like gas sensor, High electron mobility useful for transistors, low electrical conductivity. The electronic characteristics such as the band structure, DOS, PDOS, and Fermi level, of ZnO have been extensively studied using both experimental and computational techniques. Experimental studies have measured the bandgap of ZnO to be around 3.3-3.4 eV at ambient temperature, depending on the methods used for measurement. The band structure of ZnO has also been probed using techniques such as angle-resolved photoemission spectroscopy (ARPES), which has revealed the complex band plot of ZnO due to its wurtzite crystal structure.

Computational methods, such as density functional theory (DFT), are utilized to study the electronic, structural, optical, and magnetic properties of ZnO. Density of states of ZnO which provide the details about the energy levels accessible for electronic transitions, has also been computed using DFT calculations. The calculated density of states of ZnO shows a complex distribution of energy levels due to the unique electronic properties of the materials.

In addition, DFT simulations have been utilized to varify the effect of defects, such as oxygen vacancies and zinc interstitials [9-12]. On the electronic properties of ZnO. These defects can introduce additional energy levels in the bandgap of ZnO, which may significantly affect its electronic behaviour [13-17]. These different configurations affect the properties of materials like intensity of density of states (DOS) decreases if on the top of the ZnO supercell an oxygen vacancy arise. [18-20].

Properties of Zinc Oxide (ZnO)

ZnO is an inorganic compound having wide range of application due to some extraordinary physical and chemical properties [21].

Table 1.

Physical and chemical properties of ZnO.

Appearance	White powder, odourless
Chemical formula	ZnO
Crystal structure	Cubic Zinc blend, Hexagonal Wurtzite
Density	5.6 g/cm^3 [22]
Boiling point	2360°C
Melting point	1974°C [23]
Band gap	~ 3.4 eV (Direct bandgap)
Binding energy	60 meV

ZnO can react with both acid and base so it is a amphoteric oxide. Under ultra violet light it can decompose organic pollutants and produce hydrogen fuel so ZnO can be used as photocatalytic activities.

I. Structural, electronic and optical properties of ZnO

Rosely M.V.S. Almeide et.al. used Tran-Blaha modified Johnson potential (TB-mBJ) [24] a density functional theory approach for accurate electronic and optical properties within the PAW(Projected Augmented wave) [25] technique with VASP [26] software to verify the electronic, structural and optical properties of ZnO. Valence electrons of both Zn (3d, 4s) and O (2s ,2p) used

Table 2.

Lattice constants and Band gap of ZnO using conventional DFT functionals.

DFT functional	Calculated Band gap (eV)	Lattice parameters		References
		a =b (in Å)	c (in Å)	
LDA-PZ	0.7	3.276	5.279	[29]
LDA-PZ	0.794	3.186	5.150	[30]
LDA	0.759	3.184	5.177	[31]
GGA-PBE	0.830	3.275	5.309	[31]
GGA-PBE	0.67	3.312	5.322	[29]
GGA-PBE	0.74	3.259	5.218	[32]
GGA-PBE	0.83	3.250	5.207	[33]

Table 3.

Band gap of ZnO using DFT+U functional

Exchange correlation functional	Hubbard parameter $U_{d,Zn}$	$U_{p,O}$	$U_{s,Zn}$	K-point	Cutoff energy (in eV)	Band gap(in eV)	Reference
LDA+U	3	5	5	7×7×7	3265	3.32	[29]
GGA+U	5	4	4	7×7×7	3265	3.3	[29]
GGA+U	10	7	---	4×4×2	380	3.37	[34]
GGA-PBE+U	10	7	---	9×9×6	340	3.48	[35]
GGA-PBE+U	10	7	---	14×14×10	500	3.4	[36]
LDA+U	10.5	7	---	3×3×2	380	3.34	[37]
GGA-PBE+U	10	9	---	11×11×5	400	2.28	[38]
LDA+U	10	5.9	---	5×5×4	380	3.09	[39]

for the calculations with k-point 9×9×7 and cutoff energy 450 eV.

This study investigated various properties like electronic, structural and optical properties the calculated lattice parameters were lattice parameter a = b = 3.291 Å and c = 5.266 Å after geometry optimization. Which is excellent agreement with outcomes of the experimental result. The result indicate ZnO has band gap of 3.10 eV. The direct band gap was represented by the upper layer of valence band and lower later of conduction band, which occupied same line of symmetry. The density of states (DOS) represents the more contribution of valance band comes from O-2p orbitals whereas conduction band had maximum contribution of both Zn 4s and 4p orbitals [27]. In ultraviolet region ZnO exhibits strong optical absorption which is an important parameter for optoelectronic devices.

Geoffrey Tse utilized Quantum espresso (QE) algorithm to calculate the optical characteristics of ZnO using *first principle* calculation using DFT. The computations were carried out using Ultrasoft pseudopotential. The predicted lattice parameters a = b = 3.25 Å and c = 5.29 Å and band structure 3.37 eV were reported from the structural and electronic properties which are excellent agreement with the experimental findings. Using Arbi and Ambrosch-Draxl equation formalism optical properties like absorption, reflectivity, refractive index, conductivity and dielectric loss were computed. The calculation indicated the optical plots peak changes from blue to red when stress is applied. The emission peak was reported at 0.14 eV blue shift. [28].

V.N. Jafarova, G.S Orudzhev verified the electronic and structural properties of ZnO using Hubbard (U) parameters. Structural, electronic properties like, lattice parameter, DOS, band structure were calculated and plotted using *first principle* calculation based on DFT with ATK software (Atomistix Toolkit program software). Both LDA and GGA formalism was considered with

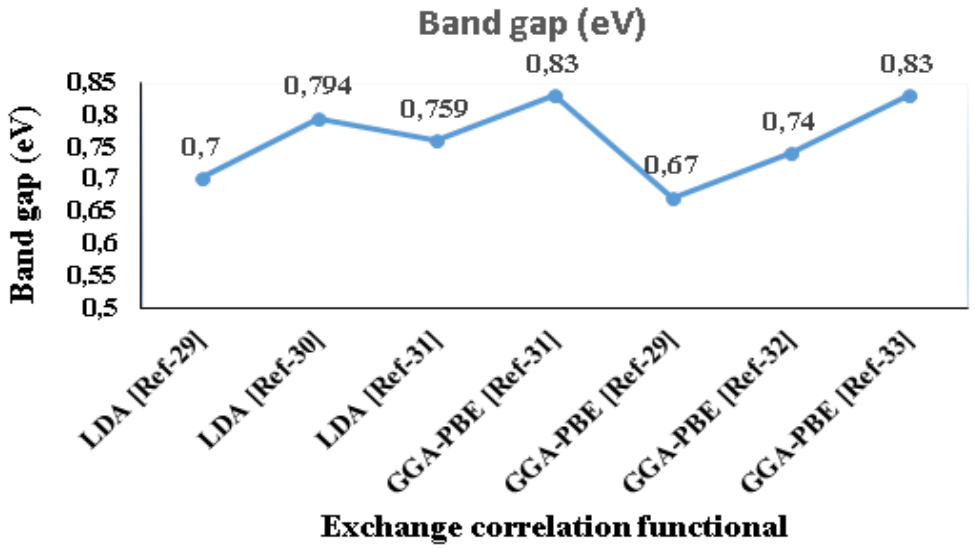

Fig. 1. Band gap of ZnO using conventional LDA and GGA exchange correlational functional.

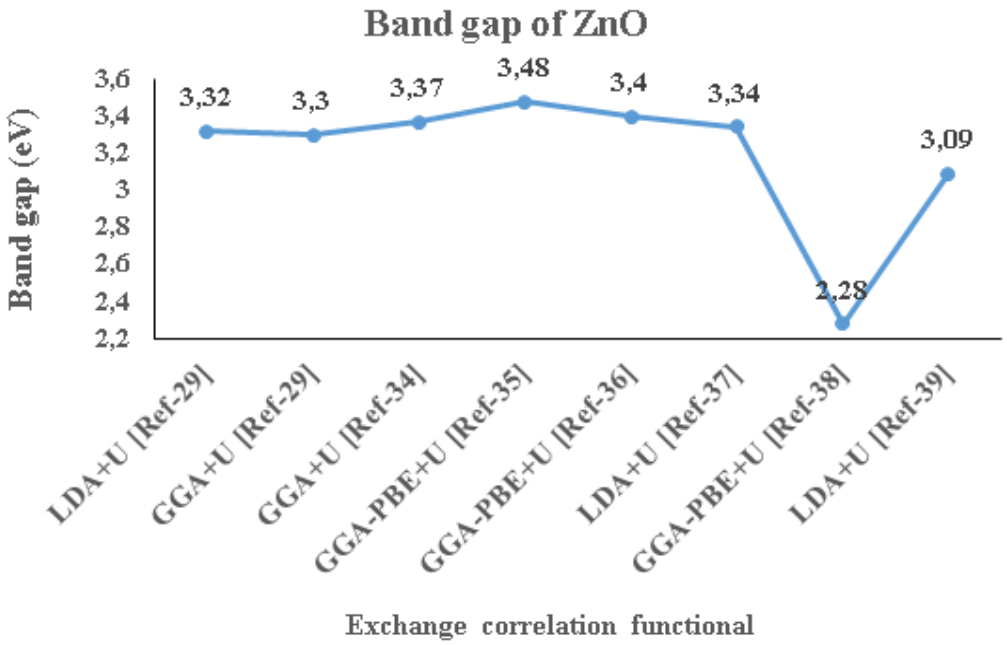

Fig. 2. Band gap of ZnO using Hubbard parameters with different exchange correlational functional.

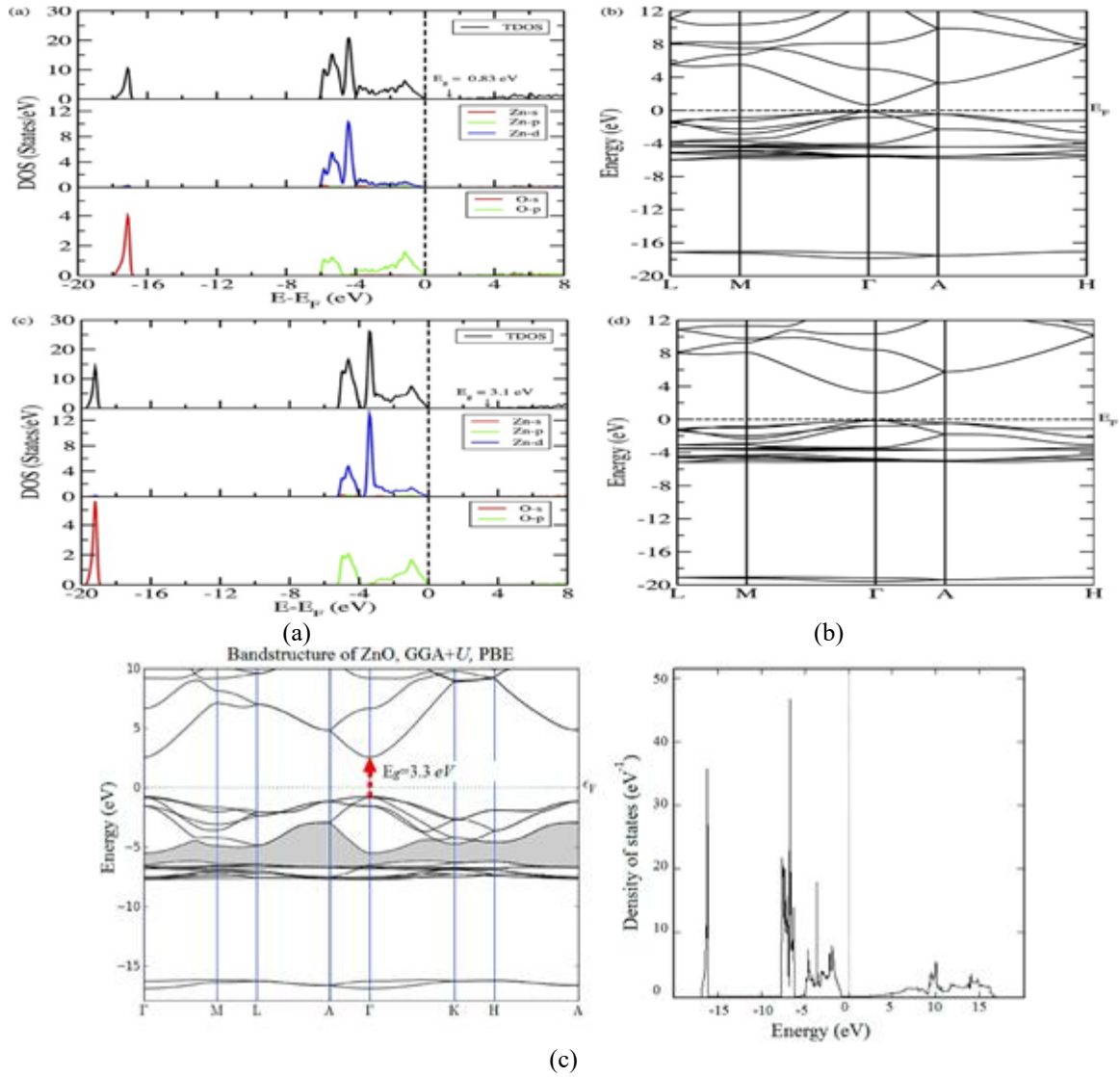

Fig. 3. Band structure, DOS, PDOS of ZnO (a) GGA-PBE formalism (upper) and TB-Mbj formalism (lower). [24], (b) LDA+U formalism, (c) GGA+U formalism [29].

different cutoff energy, for LDA formalism 3265 eV cutoff energy with K-point 7×7×7 considered whereas for GGA formalism 240 eV cutoff energy with K-point 7×7×7 was taken for the calculations. To solve the band gap problem of conventional DFT formalism Hubbard parameters were considered for the valance electrons of both Zn and O. In this calculation for LDA+U formalism ($U_{d,\ Zn}$ = 3 eV, $U_{p,\ o}$= 5 eV, and $U_{s,\ Zn}$= 5 eV) and for GGA+U formalism ($U_{d,\ Zn}$ = 5eV, $U_{p,\ o}$= 4 eV, and $U_{s,\ Zn}$= 4 eV) Hubbard values were considered. Lattice parameters and were calculated using both LDA and GGA formalism. with a = b = 3.276 Å, c = 5.279 Å and a = b = 3.312 Å, c = 5.322 Å respectively. In both formalisms the calculated band gap value (0.7 eV for LDA and 0.67eV for GGA) underestimated the experimental findings. Hubbard parameters enhanced the structural and electronic characteristics with band gap 3.32 eV for LDA+U formalism and 3.3 eV for GGA+U formalism. ZnO's electronic characteristics shows a direct band gap at the center of the Brillouin zone, as top of the valance band occupied same symmetry line with bottom of the conduction band. Zn-3d states and O-2p states showed a substantial interaction as demonstrated by PDOS calculations. Both the GGA+U and LDA+U calculation Valance band consisting of three regions with first region mainly formed from 0-2s states, middle region with Zn-3d states and nearly fermi level region with o-2p states and Zn-4s stated formed bottom of the conduction band with different energy gap range between each region. [29.]

Why group III element doped with ZnO

Improve electrical conductivity - Increasing electrical conductivity is necessary due the low conductivity of ZnO which make it challenging to use for various application including solar cell and photovoltaic applications. The electrical conductivity was increased by doping group-III materials which also have outstanding optical characteristics. Since group-III elements have fewer valance band compared to Zn, charge carriers introduced when they are doped with Zn-site of ZnO. Due to higher no of electrons Al and Ga doped ZnO introduced n-type semiconducting characteristics.

Improving stability of ZnO – ZnO that has been doped with group-III elements may have less resistance, which is relevant for transparent conductive electrodes. Additionally, it reduces formation defect of materials and increases ZnO stability.

Improving opto-electronic properties. - Doped with group-III elements has improved optical characteristics and may have shifted emission and absorption wavelengths, enabling the development of variety of ZnO based optical devices. As in indium (In) doped widen the band gap so In doped may be ideal for UV optoelectronic devices.

II. Structural and Electronic Properties of Group-III elements doped ZnO

2.1. Computational methods

Pornsawan Sikam, Pairot Moontragoom et.al. described the structural and optical characteristics of both 'Al' and 'Ga' doped with ZnO both computationally as well as experimentally. Structural and electronic characteristics like band structure, DOS and PDOS investigated using 2×2×2 ZnO supercell with Vienna-Ab initio-simulation package (VASP) [40]. Software with the help of Projected- augmented plane wave pseudopotential (PAW). To explain the total energy GGA-PBE approximation used that solve the exchange correlation potential. valence electrons d^{10} p^2 of Zn and s^2 p^4 of O preferred for the calculations with cut-off energy 400 eV and k-point 5×5×3. Zn atom substituted by Al as well as Ga atom. This study also examined Al-Ga co-doping of ZnO also investigated by substituting two Zn atom one with Ga atom and other one with Al atom [41].

Mohamed Khuili, Nijma Fazouan, et.al. described the structural, electronic, optical and electronic characteristics of 'Al', 'Ga', 'In' doped ZnO. The calculation related to DFT with Full Potential-Linearized- Augmented plane wave (FP-LAPW) using Wien2K code. [42] code using PBEsol approximation. Structural and electronic properties were Calculated using 2×2×2 supercell with Zn atom located at (1/3,2/3,0) and (1/3,2/3,1/2) and O located at (2/3,1/3,u) and (2/3,1/3,1/2+u) positions [43].

Yen- Chun peng, Chieh-Cheng Chen *et .al.* investigated the electronic and optical properties of intrinsic and Boron doped ZnO. Structural, electronic and optical properties of intrinsic and boron doped ZnO were verified using *first principle* calculations associated with DFT. Ultrasoft pseudopotential with K-point 4×4×2 were adopted for geometry optimization of ZnO. Only valance electrons were considered for the calculation. In this study 6.25% of boron atom doped with ZnO for Zn vacancy and oxygen vacancy whereas 5.88% of boron atom was doped for interstitial Zn atom of 2×2×2 ZnO supercell. Here to overcome the problem in band gap DFT+U method was used with U_d=10, U_p=7 [44].

Chieh-Cheng and Hsuan-Chung Wu investigated the structural, electronic and optical characteristics of Al-doped ZnO (Al-ZnO), Ga-doped ZnO (Ga-ZnO), and Al, Ga co-doped ZnO (Al-Ga) ZnO. Structural and optical properties of intrinsic, Al, Ga and (Al-Ga) ZnO were studied using 3×3×3 ZnO supercell. Calculations were done by using CASTEP [45] module using ultrasoft pseudopotential with K-point 3×3×2 and cutoff energy 400 eV. Valance electrons were considered for structural, electronic properties calculations. In this paper DFT+U method was adopted to overcome the problem arise related to the band gap. [46]

Mingyang Wu, Dansun *et.al.* investigated the electronic and optical properties of Al-doped ZnO bulk and ZnO monolayer for the transparent conducting material application. Structural, electronic, optical properties of Al-ZnO for both ZnO bulk and ZnO monolayer calculated based on the DFT using CASTEP with ultrasoft pseudopotential for electron and ion interaction. K-point for bulk Al-ZnO and monolayer Al-ZnO was considered 4×4×2 and 6×6×1 respectively. Different Al concentrations (6.25%, 12.5%, 18.75%) for both Bulk Al-ZnO and monolayer Al-ZnO was considered. In this work to avoid band gap problem DFT+U method was adopted with $U_{d,Zn}$= 10 and $U_{p,O}$= 7 [47].

Deping Xiong, Miao HE, *et.al* verified the electronic and optical characteristics of Boron doped ZnO. ZnO 2×2×2 supercell with interstitial boron in both octahedral and tetrahedral and boron substitution on both Zn site and O-site verified with different boron doping concentration with cutoff energy 420 eV and k-point 4×4×2 using GGA formalism. DFT+U method was implicated for accurate study of electronic and optical characteristics with $U_{d,Zn}$ = 10.5 eV and $U_{p,O}$ = 7 eV [48].

2.2. Structural and Electronic properties

2.2.1 Structural properties

Al and Ga atoms substituted on both Zn and O site of ZnO and Total energy calculated. Total energy of Ga and Al doped ZnO investigated to verify which atom whether Zn or O will be replaced by the doping element. Total energy of Ga-ZnO and Al-ZnO observed -144.831 eV and -148.327 eV respectively when doped atom replaced by Zn atom and total energy of Ga-ZnO and Al-ZnO observed -133.64 eV and -133.823 eV respectively when doped atom replaced by O atom. The calculated total energy of Ga-ZnO and Al-ZnO on Zn sites minimum compared to O sites so the doping elements replaced the Zn atoms. Lattice constants of Pure ZnO, Ga-ZnO, Al-ZnO, Ga-Al ZnO calculated [41].

The computed lattice parameter values a=b= 3.250 Å and c=5.207Å good agreement with the experimental studies. To verified the structural, electronic properties 3.125% of Al, Ga, and In doped with ZnO. The doping element affected the structural properties of ZnO, lattice constants 'a 'and 'c' values were lesser compared to intrinsic ZnO as Zn^{3+} had radius 0.74Å replaced with either Al^{3+} with radius 0.54Å and Ga^{3+} with radius 0.62Å. Band gap of intrinsic ZnO were 2.79eV [43].

Structural properties of ZnO indicates the average bond length of ZnO were 1.981Å and lattice parameters a=b= 3.249Å, c=5.232Å. Bond length of B-O was less compared to Zn-O due to the radius of Zn^{2+} (0.74Å) more than B^{3+} (0.27Å) [44].

Lattice parameters and average bond length were calculated after geometry optimization. Intrinsic ZnO were lattice parameter a=b= 3.281Å and c=5.296Å. Average bond length of (Zn-O) [2.002Å] in intrinsic ZnO was less compared to the Al, Ga, (Al, Ga) ZnO [2.009Å] whereas bond length of Al-O and Ga-O were 1.810Å and 1.907Å respectively [46].

Initially geometrically optimised the structure to calculate the Lattice constants and bond length of intrinsic

ZnO and Al-ZnO with different doping concentration. Lattice constants for intrinsic ZnO were a = b= 3.313 Å and c = 5.329 Å reported. Lattice parameters decreased with increased the Al concentration for both bulk and monolayer ZnO. Lattice parameter of Al-ZnO monolayer slightly more compared to the bulk Al-ZnO. In bulk Al-ZnO the computed lattice parameters a = b = 3.312 Å, c = 5.315 Å for 6.25% of Al doping where as a = b = 3.307 Å, c = 5.302 Å and a = b = 3.306 Å, c = 5.324 Å for 12.5% and 18.75% of Al doping respectively. Similarly, for Al-ZnO monolayer lattice parameters were calculated and observed that lattice parameters value slightly increased compared to the bulk Al-ZnO but like bulk Al-ZnO lattice parameter values decreased with increased concentration of Al doping. Calculated lattice parameters were a = b = 4.43 Å, a = b = 4.42 Å and a = b = 4.408 Å for 6.25%, 12.5%, and 18.75% of Al doping respectively. Stability of a material depends on formation energy. Material with higher formation energy are lower stability and material with lower formation energy had more stability. From formation energy calculation it was observed the formation energy values for Al-ZnO monolayer smaller compared to the bulk Al-ZnO in different doping concentration. [47]

2.2.2. Electronic Properties

Band structure indicate direct bandgap characteristics of pure ZnO as both the topmost of the valence band and

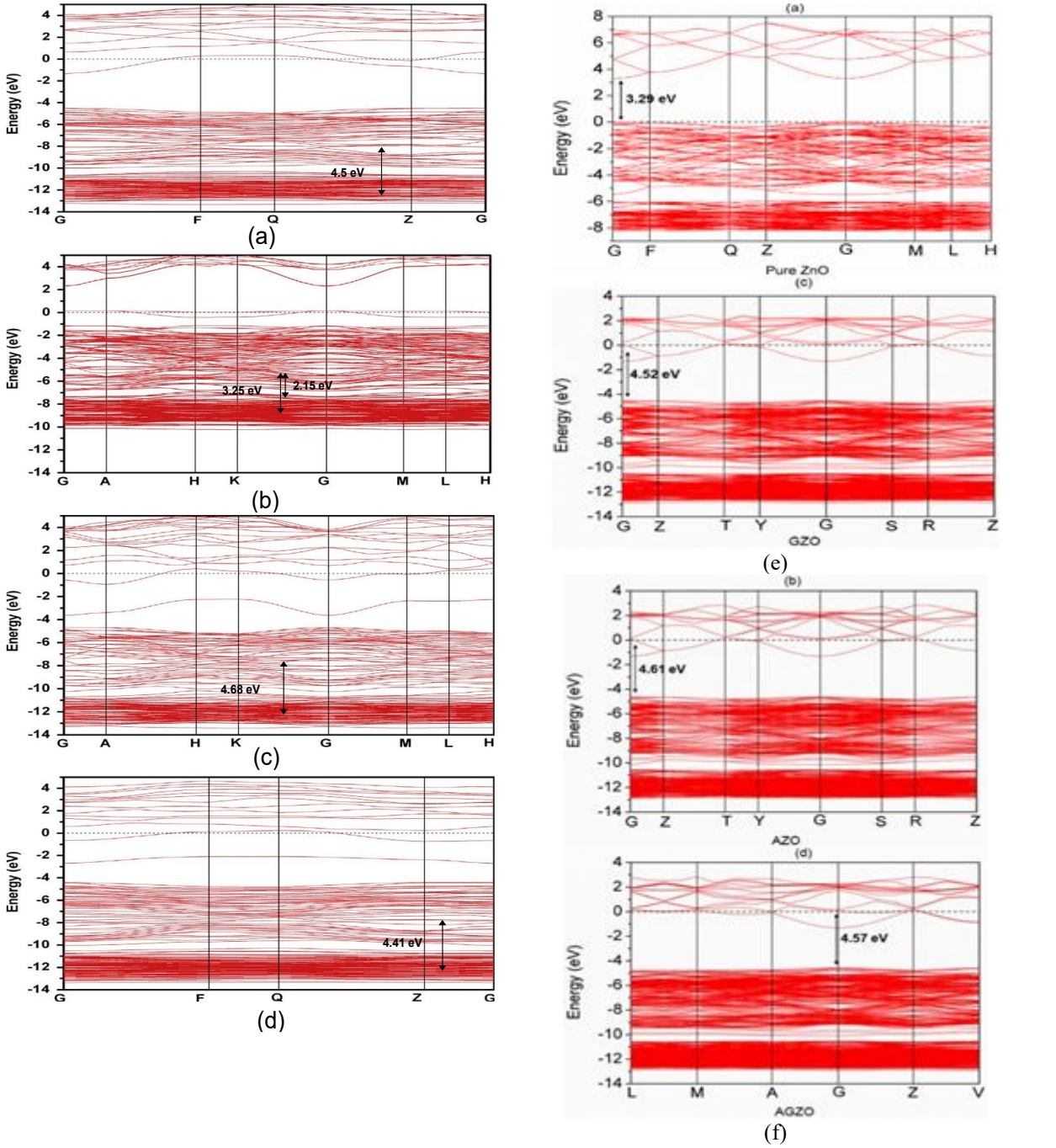

Fig. 4. Band structure of (a) Boron doped ZnO (b), Boron doped Zn vacancy, (c) Boron doped Oxygen vacancy (d) Boron doped Zn interstitial [44], (e) Band structure of Intrinsic ZnO, Ga doped ZnO, (f) Al doped ZnO, Al- Ga co-doped ZnO [46].

bottom of the conduction band occupy at same symmetry of lines i.e gamma point. The computed band energy gap of intrinsic ZnO, Ga-ZnO, Al-ZnO, (Al-Ga) ZnO were 0.76 eV, 0.53 eV, 0.60 eV, and 0.64 eV respectively. The calculated band gap is smaller compared to the experimental findings due to some limitations of DFT. However, it provided valuable information of ZnO doped with Aluminium and Gallium has a band gap that is smaller than that of the intrinsic ZnO in both situation, making it appropriate for use as a Photocatalyst.

Total density of states (TDOS) calculated and plotted using k-point 13×13×7 for intrinsic ZnO, Al-ZnO, Ga-ZnO, as well as (Al-Ga)-ZnO. From TDOS plot it was observed a shift in the fermi level towards the conduction band when Al and Ga doped with ZnO that affected the electronic properties like band gap, optical properties also thermos electric properties. The fermi level shifted towards the conduction band is due to the n-type doping of ZnO as Al^{3+} and Ga^{3+} replaced by Zn^{2+} the no of free electrons produced due to the donor state. Partial density of states (PDOS) of pure ZnO pointed out the top of the valence band is filled with 'd' states of Zn atom and p states of O atom whereas Al and Ga doped ZnO introduced another state in the valence band in Al-ZnO 'P' states of Al contributed whereas in Ga-ZnO 'd' states of Ga contributed [41].

Both the higher of the valence band and lower layer of the conduction observed at the line of symmetry. representing the direct bandgap characteristics of Intrinsic ZnO. Al, Ga, and In doping with ZnO affected the

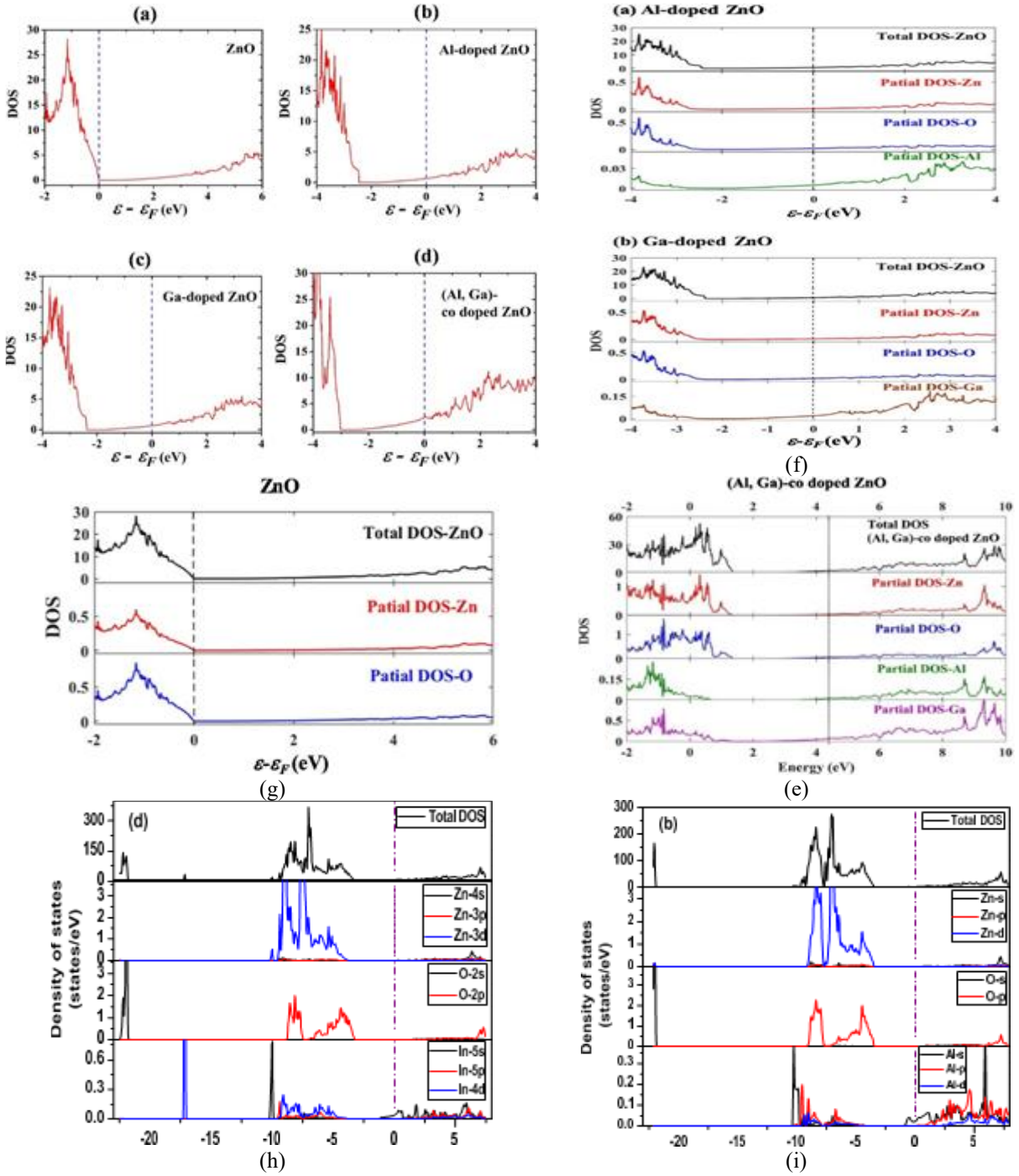

Fig. 5. (a) DOS of Intrinsic ZnO, (b) Al-ZnO, (c) Ga-ZnO, (d) (Al-Ga) co-doped ZnO, PDOS of (e) Intrinsic ZnO, (f) Al-ZnO and Ga-ZnO (g) (Al-Ga) co-doped ZnO [41]. (h) In-ZnO, (i)Al-ZnO [43].

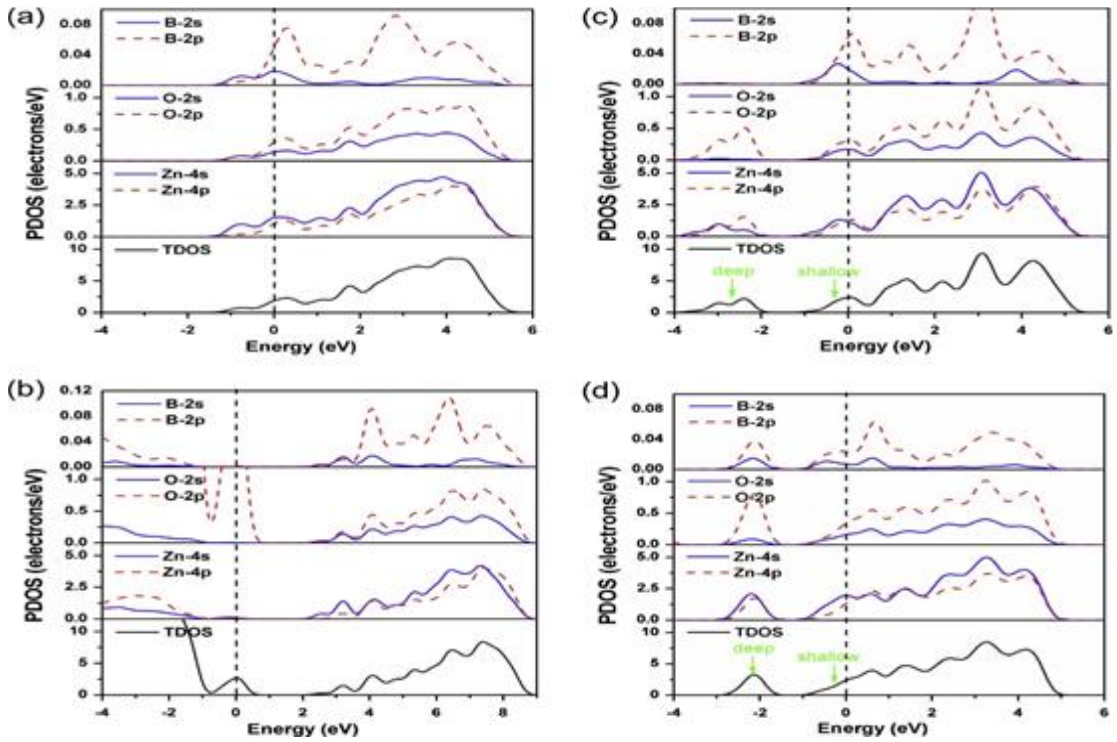

Fig. 6. DOS for (a) Boron doped ZnO (b), Boron doped Zn vacancy, (c) Boron doped Oxygen vacancy (d) Boron doped Zn interstitial [44].

electronic properties of ZnO. The fermi level shifted to the conduction band indicates the n-type nature of doped ZnO. The doping of group III element decreased the electronic band gap but widen the optical band gap due the Moss-Burstein effect [49]. The optical band gap of Al, Ga, In doped ZnO were 3.31, 3.32 and 3.18 respectively. DOS, PDOS plot of intrinsic ZnO were calculated and plotted using TB-mBJ approximation. The lower region of valance band was contributed from O-2s states whereas the higher valance band region from Zn-3d and O-2p states and Zn-4s states contributed in conduction band in case of intrinsic ZnO. In Al doped ZnO peaks were shifted towards lower energy region. Al-4s, Ga-4s and In-5s states contributed in doped ZnO [43].

Electronic properties like band structure, DOS were calculated and plotted. For intrinsic ZnO calculated band gap was 3.37 eV which is excellent agreement with the experimental findings. In boron doped ZnO (B-ZnO) one of the boron atom replaced with Zn atom. B-ZnO shifted fermi level towards the lower of conduction band from top of the valance band. Due to Burstein-moss effect doping of boron atom widen the optical band gap. DOS plot indicated conduction band minimum composed with Zn-4s, Zn-4p and small contribution also from O-2s, and O-2p states [44].

Doped ZnO with Al,Ga, and (Al,Ga) revealed n-type conductivity as the fermi level moved to the lower part of the conduction band and widening the optical band gap. Calculated optical band gap for different group-III element doped ZnO was 4.52 eV, 4.61 eV, and 4.57 eV for Ga-ZnO, Al-ZnO, (Al, Ga) ZnO respectively. DOS plot indicated the vacant donor states were contributes from Al-3s, Ga-4s, and s,p states of Zn and O. Conduction band composed with s, p states of Zn, O, Al and Ga in Al-ZnO and Ga-ZnO [46].

The uppermost valance band and the lower portion of the conduction band were found near to the Brillouin zone's gamma point, with a band gap of 3.37 eV indicating the direct band gap characteristics of intrinsic ZnO. DOS plot of pure ZnO represented the contribution of different states on valance band as well as conduction band. Maximum contribution of the Valence band maximum from 3d states of Zn atom where as 2p states of O atom contributed more on bottom of the conduction band. Calculated Band gap of pure ZnO monolayer was 4.03 eV which was larger compared to pure bulk doped ZnO. Al doped ZnO indicated the n-type semiconductor characteristics of ZnO as fermi level shifted towards the conduction band minimum. With increased the Al concentration on bulk Al-ZnO band gap value decreased but further increased the doping percentage more than 12.5% band gap value slightly increased. Where as in case of Al-ZnO monolayer below 6.25% of doping band gap decreased and the band gap value increased further the doping percentage increased [47].

The reported band gap for intrinsic ZnO is 3.36 eV. The n-type semiconducting nature of boron-doped ZnO is indicated by the fermi-level moved close to the lower of the conduction band, and this value steadily decreases as the boron doping concentration increases. Band gap value with 6.25%, 12.5% and 18.7% of boron doping concentration were computed for 3.15 eV, 3.07 eV and 2.99 eV respectively for varied percentages of doping the DOS plot showed that for intrinsic ZnO a higher valance band formed with 2p states of O atom and lower valance band with a combination of 2p states of oxygen atom and 3d states of Zn atom. 4s states of Zn atom and 4p states of Zn atom contributed the greatest to the conduction band. B-2p orbitals were also additionally incorporated into the conduction band site for of B-ZnO [48].

III. Optical and Electrical properties of Group-III element doped ZnO

Pornsawan Sikam, Pairot Moontragoom et.al. reported the optical properties of both 'Al' and 'Ga' doped ZnO both computationally aswellas experimentally.

With increase in temp electrical conductivity (σ) of intrinsic ZnO as well as Aluminium doped ZnO increases. In Aluminium doped ZnO electrical conductivity slightly more compared to pure ZnO. For Ga-ZnO, (Al-Ga) ZnO electrical conductivity reduced with temperature increases to 1000k from ambient temperature. Ga-ZnO and (Ai-Ga)-ZnO Indicated the transition of metallic character of ZnO from semiconductor nature. Thermo- electric characteristics of Al and Ga doped ZnO when compared to Undoped ZnO, Ga doped ZnO performed better, making it appropriate for enhancing thermo-electric device performance [41].

Mohamed Khuili, Nijma Fazouan, *et.al.* reported the optical and electrical properties of 'Al', 'Ga', 'In' doped ZnO.

Reflectivity, refractive index, absorption co-efficient were calculated and plotted. From imaginary part of dielectric constant indicated the first transition edge of intrinsic ZnO occurs at 2.8 eV due to transition between 2p states of the O atom valance band and 4s states of Zn atom and 4p states of Zn atom. In case of Ga-doped ZnO transition edge occur at 3.23 eV due to Ga-4s states with vacant 4s states of Zn atom and 4p states of Zn atoms formed conduction band. Al and In doped ZnO the transition edge located at 3.31 eV and 3.18 eV respectively. Transition edge of Al doped ZnO formed due to the transition between 3s states of Al atom with the vacant conduction band formed due to 4s states of Zn atom and 4p states of Zn atom.

Intrinsic ZnO indicated the absorption on visible and almost infrared light spectrum. Ga doped ZnO and Al doped ZnO reduced the absorption co-efficient compared to the intrinsic ZnO and 380 nm and 350 nm respectively for Ga-ZnO and Al-ZnO. Absorption coefficient of intrinsic ZnO remains less in UV region compared to doped ZnO. When compared to intrinsic ZnO, the reflectivity of doped ZnO decreased. In the visible light spectrum, Al doped ZnO has the lowest reflectivity and this trend persisted into the infrared. The transmittance of doped ZnO increased in visible and near infrared region compared to intrinsic ZnO. Transmittance of intrinsic ZnO

Table 4.

Average transmittance of ZnO and Group- III element doped ZnO both visible region and UV region

Structure	Visible region(400nm-800nm) (%)	UV region (200nm-400nm) (%)	References
Intrinsic ZnO	88.4	64.9	[46]
Ga-ZnO	90.6	71.2	
Al-ZnO	90.9	73.4	
(Al-Ga)- ZnO	90.8	72.8	
6.25%of Al-ZnO Monolayer	98	---	[47]
12.5%of Al-ZnO Monolayer	99	----	
Intrinsic ZnO bulk	94	-----	
Intrinsic ZnO	89.2	65.6	[44]
B-ZnO	75.6	91.1	
B doped oxygen vacancy	53.2	52	
B doped Zn vacancy	86.8	68.1	
Zn interstitial	56.9	59.2	

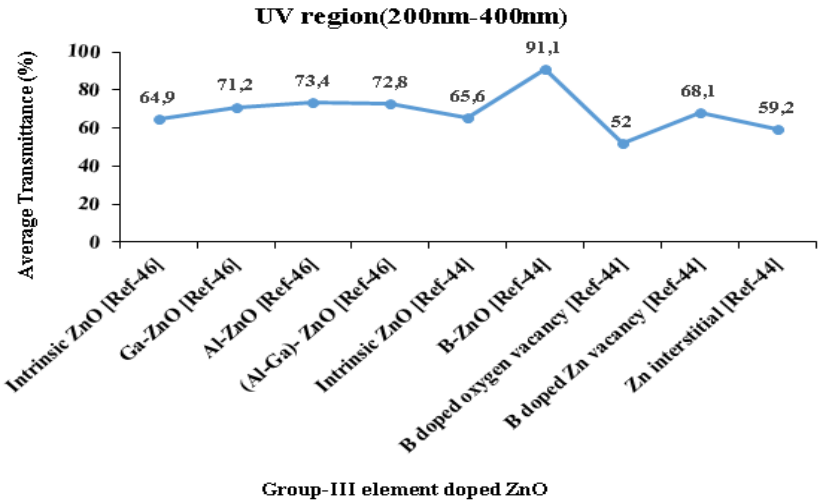

Fig. 7. Percentage of average transmittance in UV region.

starts from 440 nm whereas 334 nm, 322 nm, 315 nm for Ga, In, and Al doped ZnO respectively. Refractive index indicated the behaviour of light and refractive index decreased for doped ZnO than the intrinsic ZnO. Al –ZnO had lowest refractive index compared to In-ZnO and Ga-ZnO. Electrical conductivity of Group-III element doped ZnO increased compared to the intrinsic ZnO. High electrical conductivity occurred at Ga-doped ZnO than the Al-ZnO, and In-ZnO [43].

Yen- Chun peng, Chieh-Cheng Chen *et .al.* investigated the optical properties of intrinsic and Boron doped ZnO.

Blue shift of absorption edge observed on B-ZnO due to large optical band gap. Calculated absorption peaks for Boron doped Zn-vacancy, Boron doped O- vacancy, and Boron doped interstitial Zn were 0.3 eV, 1.5 eV, and 0.9 eV respectively. Near the fermi energy level transition of the states had lowest absorption. Transmittance of intrinsic ZnO was 89.2% on visible region and 65.6% on UV region. Transmittance for B-ZnO 91.1% on UV region, 75.6% -visible, Boron doped Zn vacancy 68.1%-UV region, 86.8%- visible, Boron doped O vacancy 52%-UV region, 53.2%- visible, and for Zn interstitial 59.2%-UV region, 56.9%- visible region were observed. Zn interstitial leads to n-type conductivity that decrease conductivity, increase effective mass and decrease mobility [44].

Chieh-Cheng and Hsuan-Chung Wu investigated optical characteristics of Al doped with ZnO (Al-ZnO), Ga- ZnO (Ga-ZnO), and Al, Ga co-doped ZnO (Al-Ga) ZnO.

Different optical properties such as co-efficient of absorption, reflection- coefficient, dielectric functions were verified. Due to the widen band gap of intrinsic ZnO no absorption occurred in visible region but Al, Ga and (Al, Ga) co-doped ZnO absorption coefficient increased than the intrinsic ZnO. Widen optical band gap of doped ZnO observed Blue-shift of absorption edge.

Transmittance of intrinsic, Al-ZnO, Ga-ZnO, (Al-Ga) ZnO were studied for both visible region and UV region. Intrinsic ZnO was average transmittance 88.4 % on visible region and 64.9% in UV region. In all the doped ZnO transmittance rate was more compared to the intrinsic ZnO both in UV region and visible region of light. Al doped ZnO had maximum transmittance compared to the Ga doped ZnO and (Al, Ga) ZnO as Al doping enhance the transmittance [46].

Mingyang Wu, Dansun *et.al.* investigated the and optical properties of Al doped ZnO for both bulk and monolayer for the transparent conducting material application.

For a transparent conducting material transmittance must be large in high wavelength range where as both reflectivity coefficient and absorption coefficient were low. optical properties result pointed out in ZnO bulk material absorption coefficient was low in both visible and IR regions but increase in UV- region. Dielectric function of pure ZnO was more compared to Al-ZnO bulk and the dielectric function of Al-ZnO monolayer even more small compared to the Al-ZnO bulk structure. Al-ZnO initially absorption coefficient decreased in visible and UV region but slightly increased at 12.5% doping concentration. Whereas absorption coefficient increased in visible region of light at 18.75 % of doping concentration. In Al doped ZnO monomer absorption coefficient decrease with increase doping concentration. Average rate of transmittance was 94% for intrinsic bulk ZnO. Transmittance in UV region and visible region of light with Al doped ZnO bulk structure and the value further increased with the more doping concentration. For intrinsic ZnO monolayer the calculated transmittance rate extremely high even compared to intrinsic bulk ZnO. Al - ZnO monolayer transmittance rate was 98 % in the visible region with increase concentration the rate of transmittance further increased and 99% for 12.5 % of Al doping but at 18.5% of Al-ZnO monolayer it decreased in UV region [47].

Deping Xiong, Miao HE, *et.al* investigated the optical properties of Boron doped ZnO.

Optical properties such as reflectivity, absorption co-efficient were calculated and plotted. In small wave length region nearly 200nm-300nm reflectivity value decreased with the increased percentage of boron doping but reflectivity value increased with percentage of doping for

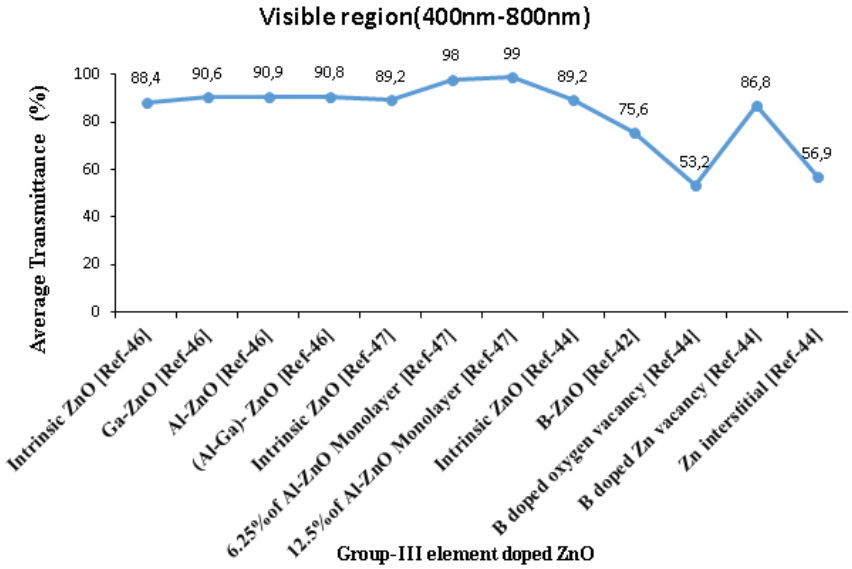

Fig. 8. Percentage of average transmittance in Visible region.

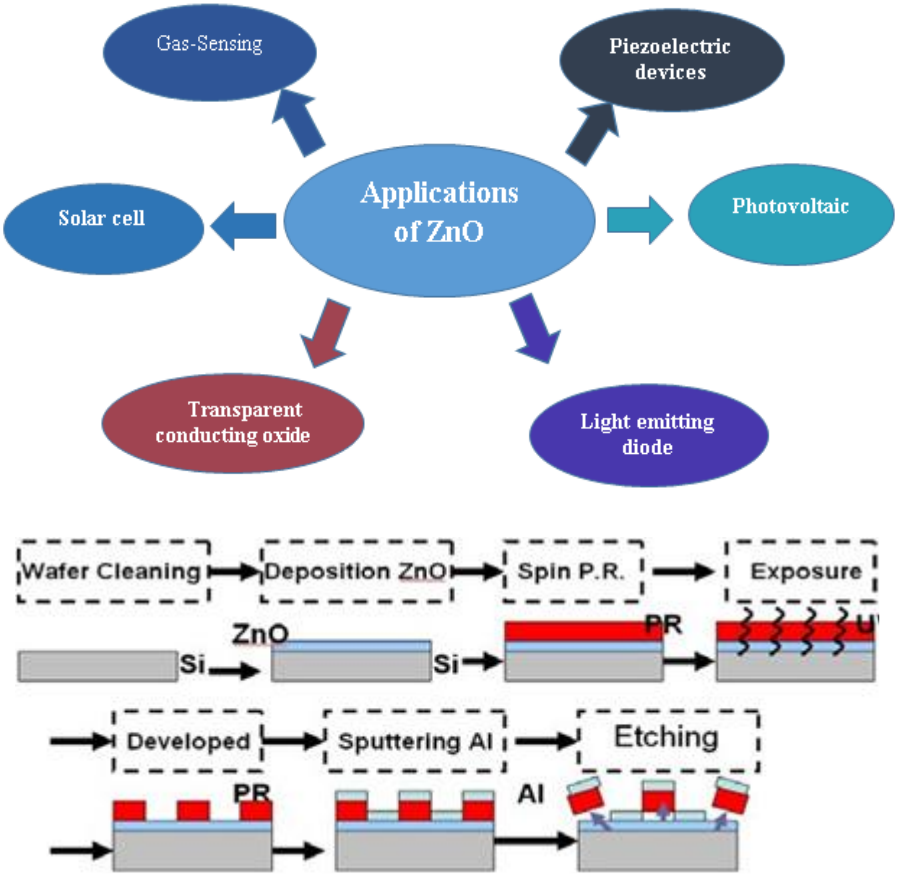

Fig. 9. Flow diagram of SAW device using ZnO thin film [52].

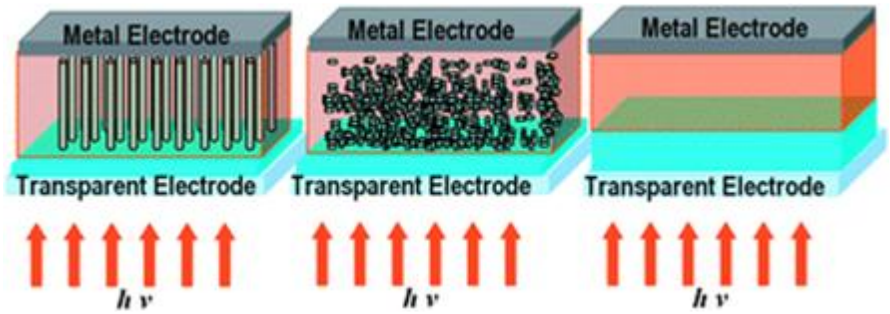

Fig. 10. Application of ZnO in hybrid and organic solar cell.

long wavelength region and less compared to intrinsic ZnO. Intrinsic ZnO indicated transmittance average greater than 90% whereas wavelength region 700-800 nm average transmittance value further increased to 95%. Boron doped ZnO increased transmittance average more than the intrinsic average transmittance value but this value decreased with the increased boron concentration as due to increased concentration of doping donor states also increased which was the main reason behind the decreased average transmittance in the wavelength range 400-1200 nm [48].

IV. ZnO device and Application

4.1. Piezoelectric device

ZnO finds widespread applications in piezoelectric devices including SAW (Surface acoustic wave) and bulk acoustic wave resonators and MSME (Micro electrochemical systems) due to extremely high electrochemical coupling coefficients [50,51,52].

4.2. Solar cell

The distinctive qualities of ZnO including its high electron mobility, transparency and outstanding electron-transport characteristics have drawn interest in the field of organic and hybrid solar cells.

ZnO frequently utilized in organic and hybrid solar cells as an electron transport layer. It is positioned between the cathode and active layer, which make it easier for electrons for producing during photon absorption to be transported efficiency due to high electron mobility. In organic solar cells ZnO can act as a buffer layer between the active layer and the transparent conducting oxide (TCO) layer. ZnO can be used as a vital component of the active layer in hybrid solar cell which integrate organic and in organic components. Specific shape and size of ZnO nano particles can improve the light absorption in the

active layer. ZnO can improve the stability of hybrid and organic solar cell by forming barrier against the elements like moisture and oxygen that might improve the efficiency of solar cell [53,54,55,56].

4.3. Light emitting diode (LED)

ZnO can be used for light emitting diodes (LEDs) specially the development of ultraviolet and visible LEDs. Electrical and optical characteristics of ZnO can be changed by doping it with impurities. For p-type doping Al, Ga and In can be used whereas for n-type doping nitrogen are the common dopant. Doping can control the conductivity of ZnO which make it good materials for LEDs.

Ultra violet photons can be produce from ZnO based LED due wide band gap. These ultra violet LED have various application in medical diagnostics. ZnO can also be used for visible LED if appropriate control of doping and fabrication process utilized. [57,58,59,60].

4.4. Gas sensing

ZnO is essential for gas sensor technology due to the special characteristics such as high surface area, chemical reactivity, photocatalytic activity and semiconducting behaviour. All these characteristics improve the sensitivity. The surface area of nanostructures like thin film, nanorods, and nanoparticles large enough to allow gas molecules to interact thus improving sensitivity. Similarly, amphoteric nature of ZnO provide it to interact with different gas molecules which improve the sensitivity. An electron hole pair produce by ZnO under ultra violet lights that electron-hole pair interact with gas molecules to improve the sensitivity, ZnO gas sensor have some advantages [61,62,63,64,65].

Low concentration of gases can be detected due to high sensitivity.

Recognises and recovers gas exposure and toxic gases quickly.

Economical production.

Minimal power consumption.

Conclusion

Overview of Group-III element-doped ZnO provided a comprehensive understanding of the notable developments and emerged as a prominent area for research with the potential for major breakthroughs and a wide range of applications in various sectors. New opportunities have been made possible by the structural, electronic, and optical properties of ZnO that can be altered and have been improved with the introduction of Group-III elements. The introduction of Group-III elements has opened up new possibilities. Extensive research has been conducted on the effects of ZnO in combination with elements such as B, Al, Ga, In. The results indicate improved stability and conductivity of ZnO. Properties of Various Group-III element doping make ZnO attractive options for different optoelectronic devices. Applications such as solar cell, LED, piezoelectric devices, photovoltaic materials, sensing, and energy storage devices. The adaptability highlights the wide range of applications and possible influence of Group-III element-doped ZnO in different field of technological advancement.

Despite the significance progress and tremendous advancement necessitating more through advancements the field of Group-III elements doped ZnO is still developing, and further study is clearly needed to fully realise its potential and resolve any obstacles. The development of unique computational techniques and deeper understanding will pave the road of the effective exploitation of the materials in real world applications. Group-III element doped ZnO transparency properties for UV region and visible region can explore more for its application in transparent conducting oxide. The utilization of novel computational methods and a great comprehension of the underlying theories are essential to advancement of this discipline. These developments will be crucial to fully realising the promise of ZnO doped with Group-III elements. The briefly further research will surely aid in the development and effective application of these materials in a variety of technological field.

Santanu Kumar Nayak – Ph.D., Assistant Professor;
Padmaja Patnaik – Ph.D., Professor;
Dipan Kumar Das – Ph.D., Assistant Professor;
Mandakini Baral – Ph.D., Assistant Professor.

[1] M. Ivill, S.J. Pearton, P.1518 D.P Norton, Jkaly, A.F. Hebard, *Magnetization dependence on electron density in epitaxial ZnO thin films codoped with Mn and Sn,* J Apple Phys, 97, P.053904 (2005).
[2] A. Das, G. Das, D. Kabiraj, & D. Basak, *High conductivity along with high visible light transparency in Al implanted sol-gel ZnO thin film with an elevated figure of merit value as a transparent conducting layer*. Journal of Alloys and Compounds, 835, 155221 (2020); https://doi.org/10.1016/j.jallcom.2020.155221.
[3] A.A. Mutalib, & N.F. Jaafar, *ZnO photocatalysts applications in abating the organic pollutant contamination: A mini review.* Total Environment Research Themes, 100013 (2022); https://doi.org/10.1016/j.totert.2022.100013.
[4] R. Kumar, O. Al-Dossary, G. Kumar, & A. Umar, *Zinc oxide nanostructures for NO_2 gas–sensor applications: A review.* Nano-Micro Letters, 7, 97 (2015); https://doi.org/10.1007/s40820-014-0023-3.
[5] M.N. Rezaie, S. Mohammadnejad, & S. Ahadzadeh, *Hybrid inorganic-organic light-emitting heterostructure devices based on ZnO.* Optics & Laser Technology, 138, 106896 (2021); https://doi.org/10.1016/j.optlastec.2020.106896.
[6] F. Rahman, *Zinc oxide light-emitting diodes: a review*. Optical Engineering, 58(1), 010901 (2019); https://doi.org/10.1117/1.OE.58.1.010901.

[7] M.K.A.A. Al-Byati, & A.M.J. Al-Duhaidahawi, *Synthesis and Characterization of Zinc Oxide Nanoparticles by Electrochemical Method for Environmentally Friendly Dye-Sensitized Solar Cell Applications (DSSCs).* Biomedicine and Chemical Sciences, 2(1), 53 (2023); https://doi.org/10.48112/bcs.v2i1.348.

[8] M. Wlazło, M. Haras, G. Kołodziej, O. Szawcow, J. Ostapko, W. Andrysiewicz, & T. Skotnicki, *Piezoelectric Response and Substrate Effect of ZnO Nanowires for Mechanical Energy Harvesting in Internet-of-Things Applications*, Materials, 15(19), 6767 (2022); https://doi.org/10.3390/ma15196767.

[9] Y. Hinuma, T. Toyao, T. Kamachi, Z. Maeno, S. Takakusagi, S. Furukawa, ... & K.I. Shimizu, *Density functional theory calculations of oxygen vacancy formation and subsequent molecular adsorption on oxide surfaces.* The Journal of Physical Chemistry C, 122(51), 29435 (2018); https://doi.org/10.1021/acs.jpcc.8b11279.

[10] D.Q. Fang, R.Q. Zhang, Y. Zhang, & S.L. Zhang, *Effect of oxygen and zinc vacancies in ferromagnetic C-doped ZnO: Density-functional calculations.* Journal of magnetism and magnetic materials, 354, 257 (2014); https://doi.org/10.1016/j.jmmm.2013.11.015.

[11] I. Ritacco, O. Sacco, L. Caporaso, & M.F. Camellone, *DFT Investigation of Substitutional and Interstitial Nitrogen-Doping Effects on a ZnO (100)–TiO_2 (101) Heterojunction*. The Journal of Physical Chemistry C, 126(6), 3180 (2022); https://doi.org/10.1021/acs.jpcc.1c09395.

[12] A. Janotti, & C.G. Van de Walle, *LDA+ U and hybrid functional calculations for defects in ZnO, SnO_2, and TiO_2.* Physica status solidi (b), 248(4), 799 (2011); https://doi.org/10.1002/pssb.201046384.

[13] F. Oba, M. Choi, A. Togo, & I. Tanaka, *Point defects in ZnO: an approach from first principles*. Science and Technology of Advanced Materials. 034302 (2011); https://doi.org/10.1088/1468-6996/12/3/034302.

[14] S. Bai, S. Chen, Y. Zhao, T.Guo, R. Luo, D. Li, & A. Chen, *Gas sensing properties of Cd-doped ZnO nanofibers synthesized by the electrospinning method*. Journal of Materials Chemistry A, 2(39), 16697 (2014); https://doi.org/10.1039/C4TA03665D.

[15] H.C. Wu, H.H. Chen, & Y. R. Zhu, *Effects of Al-impurity type on formation energy, crystal structure, electronic structure, and optical properties of ZnO by using Density Functional Theory and the Hubbard-U method*. Materials, 9(8), 647 (2016); https://doi.org/10.3390/ma9080647.

[16] P. Erhart, A. Klein, & K. Albe, *First-principles study of the structure and stability of oxygen defects in zinc oxide. Physical Review B*, 72(8), 085213 (2005); https://doi.org/10.1103/PhysRevB.72.085213.

[17] Y. Liu, Q.Y. Hou, H.P. Xu, L.M. Li, & Y. Zhang, *First-principles study of the effect of heavy Ni doping on the electronic structure and absorption spectrum of wurtzite ZnO*. Physica B: Condensed Matter, 407(13), 2359 (2012); https://doi.org/10.1016/j.physb.2012.02.030.

[18] J. Wang, Z. Wang, B. Huang, Y. Ma, Y. Liu, X. Qin,... & Y. Dai, *Oxygen vacancy induced band-gap narrowing and enhanced visible light photocatalytic activity of ZnO*. ACS applied materials & interfaces, 4(8), 4024 (2012); https://doi.org/10.1021/am300835p.

[19] L.N. Wang, X.Y. Fang, Z.L. Hou, Y.L. Li, K. Wang, J. Yuan, & M.S. Cao, *Polarization mechanism of oxygen vacancy and its influence on dielectric properties in ZnO.* Chinese Physics Letters, 28(2), 027101 (2011); https://doi.org/10.1088/0256-307X/28/2/027101.

[20] K. Wang, D. Liu, L. Liu, J. Liu, X. Hu, P. Li,... & S. Ding, *Tuning the local electronic structure of oxygen vacancies over copper-doped zinc oxide for efficient CO_2 electro reduction*. E Science, 2(5), 518 (2022); https://doi.org/10.1016/j.esci.2022.08.002.

[21] A. Moezzi, A.M. McDonagh, & M.B. Cortie, *Zinc oxide particles: Synthesis, properties and applications*. Chemical engineering journal, 185, 1 (2012); https://doi.org/10.1016/j.cej.2012.01.076.

[22] W.M. Haynes (Ed.). CRC handbook of chemistry and physics (CRC press, 2014).

[23] K. Takahashi, A. Yoshikawa, & A. Sandhu, *Wide bandgap semiconductors*. Verlag Berlin Heidelberg, (2007).

[24] F. Tran, & P. Blaha, *Accurate band gaps of semiconductors and insulators with a semilocal exchange-correlation potential.* Physical review letters, 102(22), 226401 (2009); https://doi.org/10.1103/PhysRevLett.102.226401.

[25] P.E. Blöchl, *Projector augmented-wave method.* Physical review B, 50(24), 17953 (1994); https://doi.org/10.1103/physrevb.50.17953.

[26] G. Kresse, & D. Joubert, *From ultrasoft pseudopotentials to the projector augmented-wave method*. Physical review b, 59(3), 1758 (1999); https://doi.org/10.1103/PhysRevB.59.1758.

[27] R.M. Almeida, A.L. da Rosa, T. Frauenheim, & J.S. de Almeida, *Optoelectronic properties of zinc oxide: a first-principles investigation using the Tran–Blaha modified Becke–Johnson potential*. Physica status solidi (b), 256(4), 1800380 (2019); https://doi.org/10.1002/pssb.201800380.

[28] G. Tse, *The optical and elastic properties of strained ZnO by first principle calculations*. Computational Condensed Matter, 26, e00525 (2021); https://doi.org/10.1016/j.cocom.2020.e00525.

[29] V.N. Jafarova, & G.S. Orudzhev, *Structural and electronic properties of ZnO: A first-principles density-functional theory study within LDA (GGA) and LDA (GGA)+ U methods*. Solid State Communications, 325, 114166 (2021); https://doi.org/10.1016/j.ssc.2020.114166.

[30] M.K.Yaakob, N.H. Hussin, M.F.M. Taib, T.I.T.Kudin, O.H. Hassan, A.M.M. Ali, & M.Z.A. Yahya, *First principles LDA + U calculations for ZnO materials*. Integrated Ferroelectrics, 155(1), 15 (2014); https://doi.org/10.1080/10584587.2014.905086.

[31] B. Ul Haq, R. Ahmed, S. Goumri-Said, AShaari, & A. Afaq, *Electronic structure engineering of ZnO with the modified Becke–Johnson exchange versus the classical correlation potential approaches.* Phase Transitions, 86(12), 1167 (2013); https://doi.org/10.1080/01411594.2012.755183.

[32] X. Ma, Y. Wu, Y. Lv, & Y. Zhu, *Correlation effects on lattice relaxation and electronic structure of ZnO within the GGA+ U formalism.* The Journal of Physical Chemistry C, 117(49), 26029 (2013); https://doi.org/10.1021/jp407281x.

[33] R.M. Almeida, A.L. da Rosa, T. Frauenheim, & J.S. de Almeida, *Optoelectronic properties of zinc oxide: a first-principles investigation using the Tran–Blaha modified Becke–Johnson potential*. Physica status solidi (b), 256(4), 1800380 (2019); https://doi.org/10.1002/pssb.201800380.

[34] Y.S. Lee, Y.C. Peng, J.H. Lu, Y.R. Zhu, & H.C.Wu, *Electronic and optical properties of Ga-doped ZnO*. Thin Solid Films, 570, 464 (2014).

[35] X.Y. Deng, G.H. Liu, X.P. Jing, & G.S. Tian, *On-site correlation of p-electron in d10 semiconductor zinc oxide*. International Journal of Quantum Chemistry, 114(7), 468 (2014); https://doi.org/10.12677/JAPC.2016.52007.

[36] X. Ma, Y. Wu, Y. Lv, & Y. Zhu, *Correlation effects on lattice relaxation and electronic structure of ZnO within the GGA+ U formalism.* The Journal of Physical Chemistry C, 117(49), 26029 (2013); https://doi.org/10.1021/jp407281x.

[37] L. Honglin, L.Yingbo, L. Jinzhu, & Y. Ke, *Experimental and first-principles studies of structural and optical properties of rare earth (RE= La, Er, Nd) doped ZnO.* Journal of alloys and compounds, 617, 102 (2014); https://doi.org/10.1016/j.jallcom.2014.08.019.

[38] J.Q. Wen, Y.S. Han, X. Yang, & J.M. Zhang, *Computational research of electronic, optical and magnetic properties of Ce and Nd co-doped ZnO.* Journal of Physics and Chemistry of Solids, 125, 90 (2019); https://doi.org/10.1016/j.jpcs.2018.10.014.

[39] K. Harun, M.K. Yaakob, M.F.M.Taib, B. Sahraoui, Z.A. Ahmad, & A.A. Mohamad, *Efficient diagnostics of the electronic and optical properties of defective ZnO nanoparticles synthesized using the sol–gel method: experimental and theoretical studies*. Materials Research Express, 4(8), 085908 (2017); https://doi.org/10.1088/2053-1591/aa8151.

[40] G. Kresse, & J. Furthmüller, *Efficiency of ab-initio total energy calculations for metals and semiconductors using a plane-wave basis set.* Computational materials science, 6(1), 15 (1996); https://doi.org/10.1016/0927-0256(96)00008-0.

[41] P. Sikam, P. Moontragoon, Z. Ikonic, T. Kaewmaraya, & P. Thongbai, *The study of structural, morphological and optical properties of (Al, Ga)-doped ZnO: DFT and experimental approaches*. Applied Surface Science, 480, 621 (2019); https://doi.org/10.1016/j.apsusc.2019.02.255.

[42] T. Munir, M. Kashif, W. Hussain, A. Shahzad, M. Imran, AAhmed, ... & M. Noreen, *First principles study of structural and electronic properties of Ti doped ZnO*, Journal of Ovonic Research, 14(5), 333 (2018).

[43] M. Khuili, N.. Fazouan, H. Abou El Makarim, G. El Halani, & E.H. Atmani, *Comparative first principles study of ZnO doped with group III elements*. Journal of Alloys and Compounds, 688, 368 (2016); https://doi.org/10.1016/j.jallcom.2016.06.294.

[44] Y.C. Peng, C.C. Chen, H.C. Wu, & J.H. Lu, *First-principles calculations of electronic structure and optical properties of Boron-doped ZnO with intrinsic defects*. Optical Materials, 39, 34 (2015); https://doi.org/10.1016/j.optmat.2014.10.058

[45] M.D. Segall, P.J. Lindan, M.A Probert, C.J. Pickard, P.J. Hasnip, S.J. Clark, & M.C. Payne, *First-principles simulation: ideas, illustrations and the CASTEP code*, Journal of physics: condensed matter, 14(11), 2717 (2002); https://doi.org/10.1088/0953-8984/14/11/301.

[46] C.C. Chen, & H.C. Wu, *Electronic structure and optical property analysis of Al/Ga-Codoped ZnO through first-principles calculations.* Materials, 9(3), 164 (2016); https://doi.org/10.3390/ma9030164.

[47] M. Wu, D. Sun, C. Tan, X.Tian, & Y. Huang, *Al-doped ZnO monolayer as a promising transparent electrode material: a first-principles study.* Materials, 10(4), 359 (2017); https://doi.org/10.3390/ma10040359.

[48] D. Xiong, M. He, W. Zhang, W. Zhao, Q. Wang, & Z. Feng, *Ab initio study on the electronic and optical properties of B-doped ZnO.* Journal of Optoelectronics and Advanced Materials, 21, 129 (2019).

[49] T.S. Moss, *The Photo-electro-magnetic effect in germanium and lead sulphide*. Physica, 20(7-12), 989 (1954); https://doi.org/10.1016/S0031-8914(54)80213-8.

[50] X.Y. Du, Y.Q. Fu, S.C. Tan, J. K. Luo, A.J. Flewitt, S. Maeng, ... & W.I. Milne, *ZnO film for application in surface acoustic wave device.* In Journal of Physics: Conference Series 76(1), 012035, (2007); https://doi.org/10.1088/1742-6596/76/1/012035.

[51] Y.Q. Fu, J.K. Luo, N.T. Nguyen, A.J. Walton, A.J. Flewitt, X.T. Zu,... & W.I. Milne, *Advances in piezoelectric thin films for acoustic biosensors, acousto fluidics and lab-on-chip applications*. Progress in Materials Science, 89, 31 (2017); https://doi.org/10.1016/j.pmatsci.2017.04.006.

[52] X.Y. Du, Y.Q. Fu, S.C. Tan, J.K. Luo, A.J. Flewitt, S. Maeng ,... & W.I. Milne, *ZnO film for application in surface acoustic wave device.* In Journal of Physics: Conference Series, 76(1), 012035 (2007); https://doi.org/10.1088/1742-6596/76/1/012035.

[53] J. Huang, Z. Yin, & Q. Zheng, *Applications of ZnO in organic and hybrid solar cells*. Energy & Environmental Science, 4(10), 3861 (2011); https://doi.org/10.1039/C1EE01873F.

[54] A. Wibowo, M.A. Marsudi, M. I. Amal, M.B. Ananda, R. Stephanie, H. Ardy, & L. J. Diguna, *ZnO nanostructured materials for emerging solar cell applications.* RSC advances, 10(70), 42838 (2020); https://doi.org/10.1039/D0RA07689A.
[55] R. Zahoor, A. Jalil, S.Z. Ilyas, S. Ahmed, & A. Hassan, *Optoelectronic and solar cell applications of ZnO nanostructures.* Results in Surfaces and Interfaces, 2, 100003 (2021); https://doi.org/10.1016/j.rsurfi.2021.100003.
[56] K. Keis, C. Bauer, G. Boschloo, A. Hagfeldt, K. Westermark, H. Rensmo, & H. Siegbahn, *Nanostructured ZnO electrodes for dye-sensitized solar cell applications.* Journal of Photochemistry and photobiology A: Chemistry, 148(1-3), 57 (2002); https://doi.org/10.1016/S1010-6030(02)00039-4.
[57] S.J.Pearton, & F. Ren, *Advances in ZnO-based materials for light emitting diodes.* Current Opinion in Chemical Engineering, 3, 51 (2014); https://doi.org/10.1016/j.coche.2013.11.002.
[58] P. Manzhi, R. Kumari, M.B. Alam, G.R. Umapathy, R. Krishna, S. Ojha,... & O.P. Sinha, *Mg-doped ZnO nanostructures for efficient organic light emitting diode*. Vacuum, 166, 370 (2019); https://doi.org/10.1016/j.vacuum.2018.10.070.
[59] Y.S. Choi, J.W. Kang, D.K. Hwang, & S.J. Park, *Recent advances in ZnO-based light-emitting diodes*. IEEE Transactions on electron devices, 57(1), 26 (2009); https://doi.org/10.1109/TED.2009.2033769.
[60] J.B. Kim, D. Byun, S.Y. Ie, D.H. Park, W.K. Choi, J.W. Choi, & B. Angadi, *Cu-doped ZnO-based p–n hetero-junction light emitting diode.* Semiconductor science and technology, 23(9), 095004 (2008); https://doi.org/10.1088/0268-1242/23/9/095004.
[61] Y. Kang, F. Yu, L. Zhang, W. Wang, L. Chen, & Y. Li, *Review of ZnO-based nanomaterials in gas sensors*. Solid State Ionics, 360, 115544 (2021); https://doi.org/10.1016/j.ssi.2020.115544.
[62] L. Zhu, & W. Zeng, *Room-temperature gas sensing of ZnO-based gas sensor: A review*. Sensors and Actuators A: Physical, 267, 242 (2017); https://doi.org/10.1016/j.sna.2017.10.021.
[63] T. Shaikh, & S. Jain, ZnO Nanostructure Based Gas Sensors: Critical Review Based on their Synthesis and Morphology Towards Various Oxidizing and Reducing Gases. Current Nanomaterials, 8(4), 336 (2023); https://doi.org/10.2174/2405461508666221229103713.
[64] V.S. Bhati, M. Hojamberdiev, & M. Kumar, *Enhanced sensing performance of ZnO nanostructures-based gas sensors: A review.* Energy Reports, 6, 46 (2020); https://doi.org/10.1016/j.egyr.2019.08.070.
[65] M.A. Franco, P.P. Conti, R.S. Andre, & D.S. Correa, *A review on chemo resistive ZnO gas sensors.* Sensors and Actuators Reports, 4, 100100 (2022); https://doi.org/10.1016/j.snr.2022.100100.

С.К. Наяк, П. Патнейк, Д.К. Дас, М. Барал

Покращення властивостей ZnO: комплексний огляд стратегій легування елементами III групи та практичного застосування

Університет технології та менеджменту Центуріон, Одіша, Індія, padmaja.patnaik@gmail.com

Напівпровідники з широкою забороненою зоною, такі як оксид цинку (ZnO), володіють значним потенціалом для застосування в пристроях накопичення енергії, в оптоелектроніці, газових сенсорах та інших галузях. Однак їх практичне використання часто визначається внутрішніми обмеженнями електропровідності та ширини забороненої зони, що потребує цілеспрямованої модифікації властивостей. Як ефективна стратегія подолання цих обмежень може розглядатися легування елементами III групи. Електронні властивості ZnO, зокрема ширина забороненої зони, густина станів (DOS), часткова густина станів (PDOS), магнітні властивості, а також оптичні характеристики – електропровідність, діелектричні втрати, відбивна здатність, прозорість та поглинання – зазвичай досліджуються методами розрахунків з перших принципів у межах теорії функціоналу густини (DFT).

У даній оглядовій статті розглянуто сучасні досягнення у дослідженні ZnO, а також у ZnO, легованому елементами III групи (B, Al, Ga, In). Висвітлено різноманітні перспективні застосування ZnO, зокрема в світлодіодах (LED), газових сенсорах, п'єзоелектричних пристроях та сонячних елементах. Для вивчення структурних, електронних і оптичних властивостей як чистого, так і легованого ZnO було застосовано численні теоретичні підходи з використанням різних наближень.

Ключові слова: ZnO, елементи III групи, ширина забороненої зони, DFT, розрахунки з перших принципів.